Materials Chemistry and Physics 300 (2023) 127559

Contents lists available at ScienceDirect

Materials Chemistry and Physics

journal homepage: www.elsevier.com/locate/matchemphys

Porous beta titanium alloy coated with a therapeutic biopolymeric composite to improve tribomechanical and biofunctional balance

Ernesto J. Delgado-Pujol [a], Ana Alcudia [b], Amir A. Elhadad [c], Luisa Marleny Rodríguez-Albelo [a,*], Paula Navarro [a], Belén Begines [b], Yadir Torres [a]

[a] Departamento de Ingeniería y Ciencia de los Materiales y del Transporte, Escuela Politécnica Superior, Universidad de Sevilla, 41011, Seville, Spain
[b] Departamento de Química Orgánica y Farmacéutica, Facultad de Farmacia, Universidad de Sevilla, 41012, Seville, Spain
[c] Department of Pre-Clinical Oral Health Sciences, College of Dental Medicine, Qatar University, Qatar

HIGHLIGHTS

- Novel beta porous titanium implant coated with therapeutic biocomposite.
- Bio-functional antibacterial behavior of PVA/PCL/AgNPs biocomposite.
- A solution to improve the tribomechanical and biofunctional behavior of metal implants.

GRAPHICAL ABSTRACT

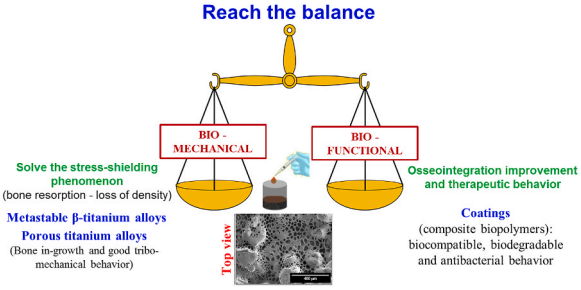

ARTICLE INFO

Keywords:
Porous beta titanium alloy
Biopolymer PVA/PCL
Silver nanoparticles
Antimicrobial activity
Tribo-mechanical behavior

ABSTRACT

Tooth loss is common in patients struggling with dental cavities, periodontal diseases, and tumors, as well as those who abuse tobacco or drugs. In this scenario, dental implants have become the primary treatment option for complete or partial tooth loss. Dental implant failure can be caused by stress shielding phenomenon, poor osseointegration, or to bacterial infections. In the present study, a joint solution to these limitations is proposed using a variety of porous β-titanium substrates using powder Ti35Nb7Zr5Ta alloy and employing the spacer-holder approach (ammonium bicarbonate) to obtain a variety of porosity percentage (30, 40, and 50 vol%), and pore diameters in 100–200 μm, that has been characterized in terms of its size distribution, density, morphology, chemical composition, compaction ability and Vickers micro-hardness. Furthermore, porosity, microstructure (Archimedes and image analysis) and tribomechanical behavior (P-h curves and scratch tests) experiments were performed to study and characterize the porous substrates. Polyvinyl alcohol (PVA)/poly-ε-caprolactone (PCL) containing silver nanoparticles (AgNPs), as antibacterial composite, was employed to infiltrate β-Ti disks. Scanning electron microscopy was used to determine the coating morphology, thickness, and infiltration of the porous substrates. Wettability and SBF experiments were also carried out to investigate hydrophobicity and potential bio-functionality. The results suggested how the porosity of the β-Ti alloy affects the mechanical characteristics and the wettability of the substrate that was successfully infiltrated to exert an antimicrobial behavior.

* Corresponding author.
E-mail addresses: erndelpuj@alum.us.es (E.J. Delgado-Pujol), aalcudia@us.es (A. Alcudia), aelhadad@qu.edu.qa (A.A. Elhadad), lralbelo@us.es (L.M. Rodríguez-Albelo), pnavarro@us.es (P. Navarro), bbegines@us.es (B. Begines), ytorres@us.es (Y. Torres).

https://doi.org/10.1016/j.matchemphys.2023.127559
Received 14 October 2022; Received in revised form 24 February 2023; Accepted 27 February 2023
Available online 3 March 2023

1. Introduction

Around 3.5 billion people worldwide suffer from oral health problems, and 267 million people are estimated to have lost teeth [1–3]. Patients' dental health and functions may be restored due to the success of dental implants, which had a global market potential of USD 4.3 billion in 2015 and is anticipated to reach USD 5.9 billion by the end of 2022 [4,5]. Dental caries, infections, and trauma are the three most frequent causes of tooth loss [6,7]. Loss of teeth may have an impact on oral health, which can cause problems with speech and chewing [8,9]. In this context, the primary treatment option for whole or partial tooth loss in this situation is dental implants [10]. Ti and its alloys, which are frequently used as long-term implants in clinics due to their improved biosafety, are preferred over stainless steels or Co-Cr alloys [11,12]. Due to its excellent biocompatibility, superior mechanical properties, and high corrosion resistance, Ti and its alloys are the materials most commonly used to produce medical and dental implants [11,12]. However, most commercially available titanium implants are solid structures; compared to bone tissue, the dense titanium has a higher elastic modulus, resulting in a larger stress shield, and promotes bone tissue resorption [13]. Furthermore, it is of great concern that the well-known primary metallic biomaterial Ti-6Al-4V alloy, which is used to build orthopedic implants, may release toxic aluminium and vanadium ions [14,15]. These ions have the potential to cause long-term health problems such as osteomalacia, Alzheimer's disease, and peripheral neuropathy [16,17]. Despite the low failure rates of these titanium implants, 5–10% of them are still known to fail (due to poor osteogenesis and infection associated with implants) and require removal [18–20]. Therefore, it is essential to create biomaterials with adequate biomechanical aspects (stiffness, mechanical and fatigue resistance), as well as a bifunctional balance (corrosion resistance and bone ingrowth), in order to manage and prevent the high rate of implant-related infections [21–23]. As a result, porous titanium implants were created with adequate biomechanical aspects that approximate bone tissue and reduce the effective stress-shielding phenomenon [24,25]. The limitations mentioned above of conventional titanium implants could be addressed by the fabrication of porous titanium alloys with appropriate mechanical properties, adequate pore sizes that are suitable for bone ingrowth and vascularization, and a lack of vanadium and aluminium ions [26]. For instant, the porous titanium produced using space-holder methodology can allow cell adhesion and growth, promoting bone ingrowth and enhancing osseointegration [20,23,27–29]. However, it is important to keep in mind that a bacterial biofilm could proliferate on the surface of a porous titanium implant with consequent implant failure [30,31]. In this scenario, an appropriate antibacterial coating might be a strategy to reduce the risk of infection while simultaneously serving as a reliable local drug delivery matrix system, improving implant biocompatibility, or strengthening corrosion resistance. It has been established that the antibacterial properties of positively charged silver ions (Ag+) make it effective against bacteria, fungi, and some viruses [32–34]. Positively charged silver ions will produce reactive oxygen species (ROS), which can facilitate the catalytic oxidation of bacterial components [35,36]. The application of silver in the form of nanoparticles (AgNPs) could combine the antimicrobial effect of both Ag+ and a nanoparticulate material. Dental coatings should preferably be mechanically stable, biocompatible, and antimicrobial [37,38]. Polymeric coatings have a significant effect on the development of modern biomaterials in the biomedical field. They can be used to enhance bioactivity, surface functionality, and wear and corrosion resistance [29,39,40]. Polyvinyl alcohol (PVA) is a hydrophilic polymer with exceptional film-forming abilities, high crystallinity, non-toxicity, and impressive chemical resistance. It also exhibits highly important functional qualities, such as high mechanical strength [41]. The PCL polymer, on the other hand, is well known for its excellent mechanical properties, cytocompatibility, non-toxicity, and slow biodegradability [42,43]. However, due to its hydrophobic nature, which hinders cell adhesion and proliferation, it is difficult to adhere to the native bone tissue [42,43]. This restriction can be overcome by combining PCL with hydrophilic polymers, like PVA. The combination of both polymers PVA/PCL could act as a polymeric biocompatible matrix that could easily be loaded with antibacterial AgNPs nanoparticles. To simulate osteo-conductance and achieve mechanical strength, it is necessary to fill the bone defects left behind after the surgical removal of benign bone tumors. Implanting porous titanium alloy coated with polymeric PVA/PCL/AgNPs into bone defects can offer a favorable bone substitute for human osteogenesis and could be a useful replacement for bone graft in the treatment of some benign tumors.

The use of β-titanium alloys (β-Ti), with Young's modulus (60–80 GPa) [44,45] that are closer to that of natural bones, is another potential solution to reduce the problem of stress-shielding [46–48]. Moreover, β-Ti exhibits improved fatigue resistance and biocompatibility [49,50]. Therefore, the capacity to balance biomechanical and biofunctional behaviors is significantly increased by the combination of porosity and β-Ti, which also boosts implant success [51]. The literature has reported on the macro-mechanical behavior of the dense Ti35Nb7Zr5Ta alloy [47,52], however there are few studies on the porous structures of β-Ti alloys [20,53]. In this study, we suggest addressing three issues related to metallic implants at once: 1) the stress-shielding of tensions, 2) avoiding the use of toxic elements (V and Al), and 3) the proliferation of bacteria.

In this research work, we propose an optimal fabrication of porous β-titanium disks using powder Ti35Nb7Zr5Ta alloy, via the accessible spacer-holder approach, to obtain a varied porosity volumes and pore diameters, to avoid the phenomenon of stress shielding. For adequate biomaterial infiltration with total pore coverage and to evaluate the potential of this methodology to fabricate implants with enhanced osseointegration and antibacterial properties, a biocompatible and non-toxic composite based on the combination of PCL and PVA, containing AgNPs was suggested.

2. Materials and methods

This section lists the materials used in the research as well as the experimental procedures that were followed to create the porous β-Ti substrates, the synthesis of the PVA/PCL/AgNPs composite, the infiltration of the porous β-Ti substrates and other critical studies for characterization (both before and after being coated with the biopolymer). The following Fig. 1 summarizes a schematic workflow including the most important details.

2.1. Materials

To fabricate the porous metal substrates, β-Ti powder was used with the stoichiometric chemical formula Ti35Nb7Zr5Ta (TNZT), (Ercata GmbH in Chemnitz, Germany). Ammonium bicarbonate (NH_4HCO_3), 99% purity, supplied by Cymit Química S.L. (Barcelona, Spain), 100–200 μm in size, was used as spacer particles. All chemical products were used directly from suppliers without any need for purification. Polyethylene glycol 3000 (PEG 3000), polyethylene glycol 200 (PEG 200), polyvinyl alcohol (PVA, Mn = 30.000–70.000 g/mol, 87–90% hydrolyzed), poly-ε-caprolactone (PCL, average Mn 80,000 g/mol), and glycerol were purchased from Sigma-Aldrich (Madrid, Spain). Silver nitrate ($AgNO_3$) was purchased from Sigma-Aldrich (Madrid, Spain). Dichloromethane and HCl (35%) were acquired from Scharlau in Barcelona, Spain, and Honeywell in Badalona, Spain, respectively. For the preparation of the solutions required by the titration method for the evaluation of bioactivity, sodium chloride (NaCl, BioXtra) ≥ 99.5% purity, di-sodium hydrogen phosphate dehydrated ($Na_2HPO_4{\cdot}2H_2O$, EMPROVE® ESSENTIAL Ph Eur, BP, USP), calcium chloride ($CaCl_2$) 97.0% purity, and Trizma base 99% purity (TRIS) were purchased by Sigma-Aldrich (Madrid, Spain).

2.2. Characterization of the β-Ti alloy powder

In this work, the morphology, size distribution, chemical composition, and other characteristics of the starting powder were all evaluated. The size distribution of the TNZT-alloy powder was measured by laser diffraction (Mastersizer 2000, Malvern Panalytical Ltd, Malvern, UK). Furthermore, a helium pycnometer (5200e, Quantachrome, Anton Paar GmbH, Graz, Austria) was used to measure the density of the powder. Using an X-ray diffractometer (XRD) (X'Pert Pro MPD, Panalytical Ltd., Malvern, UK), equipped with a goniometer and X'cellerator detector, the crystallinity was evaluated. Cu-K radiation was used to acquire the diffraction patterns in a step-by-step scanning process, with an angle variation of 0.03° and a scanning time of 300 s per scan, in the range of 2-angles from 10° to 120°. Chemical composition was assessed using an Energy Dispersive X-ray (EDX) detector and a Scanning Electron Microscopy (SEM) (Hitachi S-4800, Bruker, Billerica, Massachusetts, USA) with an electron acceleration voltage of 20 kV. The SEM images of the metal (β-Ti) particle were captured using secondary electrons at a 5 kV acceleration voltage. Finally, at least 10 Vickers microhardness measurements (HV0.01) were made using a Shimadzu HMV-G indenter (Kyoto, Japan).

On the other hand, the potential bioactivity evaluation of the β-Ti alloy powder in vivo was carried out using a rapid *in vitro* protocol mainly based on the determination of the calcium phosphate nucleation onset point associated with a pH evolution, recently described by Zhao et al. [56]. A calcium solution was added dropwise (0.1 mL/min) using a 1 mL syringe to 50 mL of phosphate solution, maintained under stirring, containing 0,1 g of β-Ti alloy powder and without the testing material for the blank-control comparison. Calcium phosphate nucleation was monitored until it took place, using a pH electrode (pH 50+DHS Set bench meter incl. pH-electrode 201T, Dostmann Electronic GmbH, Germany). During the experiment, the temperature was controlled at 25.0 ± 1.0 °C or 26.0 ± 1.0 °C. The initial pH of the solution was experimentally measured and was 7.45 and was monitored in situ using the pH electrode.

2.3. Fabrication and characterization of porous β-Ti substrates using the space-holder technique

The β-Ti powder was mixed with different spacer contents (30, 40 and 50 vol% and size range between 100 and 200 μm). To ensure that the mixtures were well homogenized, the mixtures (Ti-β + vol% NH_4HCO_3) were stirred in a Turbula T2C mixer (TMG machines, Birmingham, UK) for 40 min. The mixtures were then pressed at 800 MPa in a cylindrical 12 mm diameter die using a Universal Instron 5505 machine (Instron, High Wycombre, UK). Prior to the sinterization, removing the green disks' spacers particles was necessary. This was accomplished by two stages of thermal treatment: the first 10 h at 333 K, followed by another 10 h at 383 K under low vacuum (10^{-2} mbar) conditions. The final sintering was completed over the course of 2 h at 1673 K in a high vacuum atmosphere (10^{-5} mbar) in a molybdenum-chamber furnace from Termolab-Fornos Electricos, Lda., Gueda, Portugal. To preserve the proportion, size, and morphology of the pores, the obtained disks surface (12 mm in diameter and 4 mm high) was subjected to an appropriate grinding and polishing process. To examine the degree of infiltration of the composite biopolymer and the thickness of the coating, a comparable metallographic preparation was also performed on the cross-sectional surface of some cut disks (D-shaped substrates).

The density (ρ), as well as the total (P_T), and interconnected (P_I) porosity of the β-Ti substrates were obtained by the Archimedean method. The equivalent diameter (Deq) and the form factor (*Ff*) were evaluated from at least 10 images obtained using an optical microscope (Nikon, Tokyo, Japan), which has a "Jenoptik Progres C3" camera attached (Jenoptik, Jena, Germany) handled by the image analysis computer software "Image-Pro-Plus 6.2". The wettability test was carried out on the "Phoenix 300″ equipment (Surface Electro Optics, South Korea) following the protocol that establishes that the drop must be formed in the syringe tip and deposited on the surface [55]. The wettability of the surfaces of the titanium disks is evaluated by measuring the angle formed between the drop and the surface, using photographs captured "Phoenix 300″ equipment (Surface Electro Optics, South Korea). Using the captured images and the "Surfaceware 7″ software, the angle formed between the drop and the surface was measured.

On the other hand, the tribo-mechanical characteristics of the porous substrates were assessed using: 1) instrumented micro-indentation (load and uloading tests, P-h curves), and 2) scratch tests. Both tests were carried out using a MTR3750-50/NI equipment (Microtest S.A., Madrid, Spain). The P-h curves were performed using a Vickers indenter with a load control of 2 Nmin-1, a maximum load of 2 N, and a maintenance time of 15 s. Using the Oliver–Pharr method, the values for microhardness and Young's modules were estimated using P-h curves [56–58].

These results were corrected, considering the geometry of the indenter, as well as the wear and/or possible damage caused by its use.

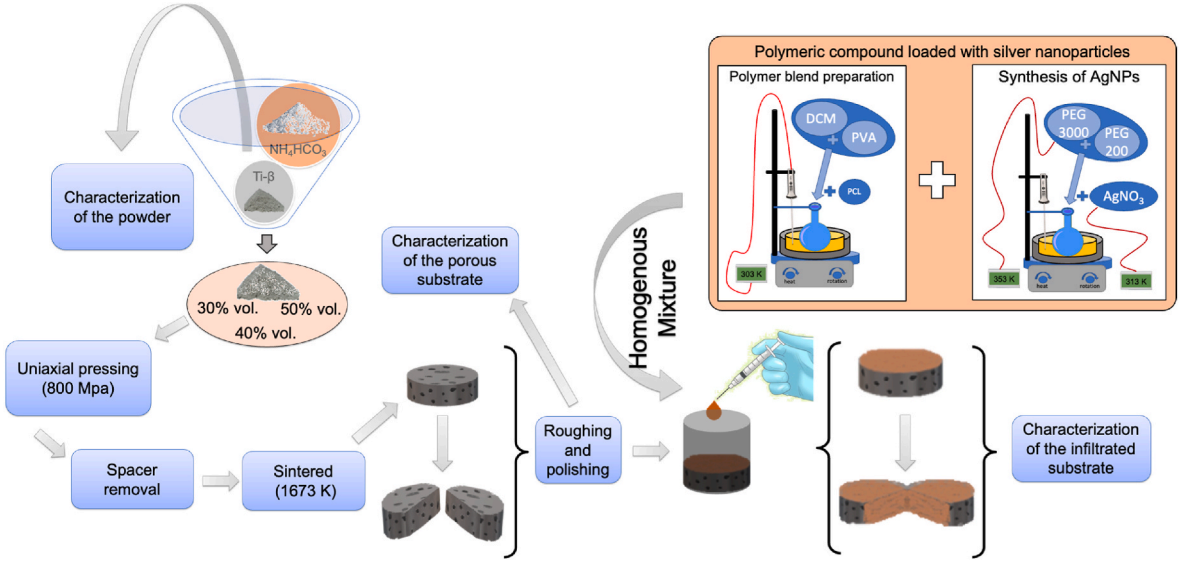

Fig. 1. Illustration of the fabrication and characterization of biopolymeric composite-coated β-Ti based porous disks.

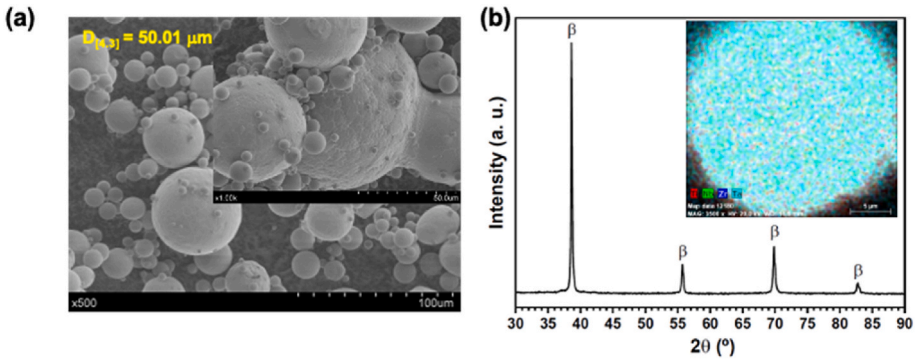

(c)

Density (g/cm^3)	HV 0.01	Chemical Composition (Wt.)		
		Element	Nominal	EDX
5.7453 ± 0.0035	154.4 ± 12.3	Ti	46 - 63	55.78 ± 0.98
		Nb	30 - 40	34.28 ± 0.85
		Zr	4 - 8	6.34 ± 0.20
		Ta	3 - 6	3.55 ± 0.04

Fig. 2. Characterization of the Ti- alloy's starting powder: Ti35Nb7Zr5Ta. a) SEM image of the powder, b) XRD diffraction pattern and SEM chemical composition mapping, c) Density and EDX analysis.

On the other hand, the scratch tests were carried out using a 200 µm diameter Rockwell diamond tip, carried out at a constant load of 3 N (rate of 0.5 mm·min-1) and a scar length of 3 mm [59]. The typical load, penetration depth, and scar length are all measured continually. The surface roughness profile during the 3 mm scar length and a negligible applied stress must be known prior to completing the scratch tests. This study allowed obtaining the characteristic roughness parameters: arithmetic mean roughness (R_a), root-mean-square roughness (R_q), maximum height from peak to valley of all the measurement trace (R_y) and arithmetic average of the maximum height from peak to valley of the roughness values of five consecutive sampling sections on the filtered profile (R_z), as well as to correct the scratch curves (considering the inclination y/or previous surface roughness). After the in-situ scratch tests were completed, a post-palpation was performed to measure the depth of permanent penetration, the elastic recovery, and the depth of groove scar roughness. Finally, an optical microscopy study of the scratch was performed, which allowed identification of potential damage mechanisms. In this work, all P-h curves and scratch tests were performed at least three times.

2.4. Synthesis and antimicrobial behavior of the biopolymer composite

According to the process described by Madhavan et al. [60], the AgNPs were synthesized, producing nanoparticles with comparable properties (spheroidal shape and approximate size of 20 nm). The procedure was carried out on a hot plate with magnetic stirring (MR Hei-Standard magnetic stirrer from Heidolph Instruments, Germany) where 10 ml of PEG 200 and 3.42 g of PEG 3000 were mixed at 353 K under constant magnetic stirring (2400 rpm). Once homogeneous, the temperature was changed to 323 K, and 100 mg of $AgNO_3$ were added, keeping magnetic stirring until a brown solution was obtained. On the other hand, to obtain the mixture of 2 g of PCL and PVA, they were prepared in a 50/50 w/w ratio on a hot plate with a magnetic stirrer. It started by dissolving the PVA in 15 ml of dichloromethane under magnetic stirring at a temperature of 303 K; Once dissolved, the PCL was added, maintaining stirring until the latter was also completely dissolved. Finally, the composite was prepared from the mixture of PCL and PVA; and addition of the previously described AgNPs to maintain a ratio of 0.4% w/w Ag.

On the other hand, the antimicrobial behavior of the used composite was described against reference bacteria strains *Pseudomonas aeruginosa* (*P. aeruginosa*, ATCC 15692), as Gram-negative bacteria, and *Staphylococcus aureus* (*S. aureus*, ATCC 29737), as Gram-positive bacteria, according to Alcudia et al. [24] work and following a modified version of the Kirby-Bauer disk diffusion method [61]. Briefly, TSA agar petri dishes were streaked with 100 or 150 µl of inoculant containing *P. aeruginosa* and *S. aureus*, respectively. 8 mm diameter cylinders of the composite were placed on top of the plates, including a gentamicin disk, as the positive control. Inhibition halos were measured after 24 h of incubation at 37 °C.

2.5. Infiltration and coating of the porous β-Ti substrates

During this process, the polished surface of the porous β-Ti disks, whole and cut into two half-moons (D-shape), were covered with biocomposite (see details of the entire process in Fig. 1). Before depositing the coating, the entire disks or the two D-shape parts, facing each other, were introduced into a heat-shrinkable rubber tube. The biopolymer composite was then deposited by dripping 300 µL of suspension with a syringe. The use of this shrinkable rubber prevents the loss of the biocomposite, covering the entire surface, and infiltrating the pores of the substrates. Finally, the coated disks were placed for 24 h in an oven at a temperature of 314 K, to evaporate the dichloromethane (solvent used in the synthesis). The use of D-shape disks enables to approach the study of the cross section of the coated disks (measure the thickness), minimizing the risks of damage to the coating in the cutting processes.

In relation to the characterization of the coated substrates, the morphology, thickness, and degree of infiltration of the composite biopolymer deposited on the porous β-Ti substrates were studied using scanning electron microscopy images (FEI TENEO, Term Fisher Scientific), obtained in secondary electron scanning mode, SEM and backscattered electrons, BSE (detect potential differences in the chemical composition of the composite biopolymer). This study was carried out on the surface and cross section of porous disks. Finally, the wettability of the surface covered with the composite biopolymer was evaluated, following the protocol already detailed.

3. Results and discussion

In this section, the results of the characterization of the β-Ti alloy powder are presented first. The following aspects of the powder were examined: its morphology, size distribution, density, micro-hardness,

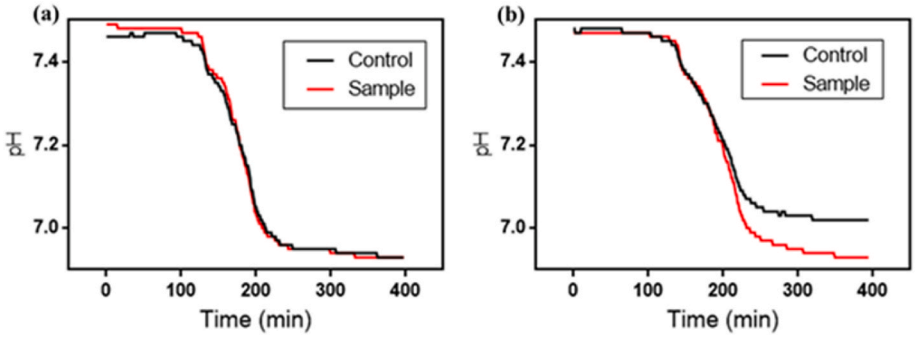

Fig. 3. Bioactivity *in vitro* test based on calcium phosphate nucleation of the β-Ti alloy powder at a) 26 °C, and b) at 25 °C.

phases, and chemical composition. Next, the porosity of the substrates is characterized, and the static behavior (P-h curves) and dynamic behavior (scratch tests) are evaluated. Finally, the appearance of the biopolymeric coating, its adherence, and degree of infiltration in the porosity of the metallic substrate are characterized. To discriminate the role of the macro-porosity inherent to the spacer and the role of the coating, the wettability of the porous disks is also tested in this work before and after coating. Finally, the antimicrobial behavior of the coating and potential β-Ti bioactive surface studies were compiled and discussed.

3.1. Characterization of β-Ti powder

In Fig. 2, some results related to the microstructural and mechanical characterization of the Ti35Nb7Zr5Ta alloy powder are summarized. The SEM images (Fig. 2a) revealed the spherical morphology of the powder, as well as its surface roughness. The diffraction pattern confirmed the presence of only β phase, with BCC cubic symmetry and space group Im-3m (Fig. 2b). The chemical composition by weight of the metallic particles coincided with the nominal values reported by the powder supplier (see table, in Fig. 2c), and the acquired composition maps showed a homogeneous distribution of the four metallic constituents in the powder (Fig. 2b). Fig. 2. c includes the value of the powder density, the Vickers micro-hardness; as well as the elemental analysis using EDX.

In relation to the calcium phosphate nucleation, an *in vitro* test of the β-Ti alloy powder would assume hydroxyapatite (HA) formation, since it is a stable biological mineral that triggers osteoblast activity for bone ingrowth. However, unfortunately, most studies are based on long time experiments that employ ISO 23314:2014, with samples immersed in SBF (simulated body fluid) for 28 days. Thus, investigating whether a material such as powder β-Ti could potentially induce superficially HA growth, is a determining factor to estimate its ability to easily promote osseointegration. In this sense, the method described by Zhao et al. [54] seems a quicker and interesting alternative to assess the generation of HA in a few hours. This method is supposed to correlate the evolution of the pH of a phosphate solution by comparing a material to determine the calcium phosphate nucleation onset point. The results obtained in the *in vitro* test for the qualitative evaluation of the ability of the β-Ti alloy powder to initiate the HA nucleation are graphically reported in Fig. 3.

The pH evolution profile was determined initially at 26 °C (Fig. 3a) and repeated at 25 °C (Fig. 3b). From these results, the critical role of temperature was observed. Indeed, a distinct visible variation of slope in the evolution of pH, that corresponds to a sudden decrease in available free Ca^{2+} for the sample, was monitored for both experiments. However, in both cases, the decrease of pH, related to the formation of octacalcium phosphate or HA, occurred simultaneously in the sample and in the blank. Therefore, no unequivocal conclusions regarding the osteointegration bioactivity behavior of the β-Ti compared to c. p. Ti could be stablished, requiring further and more deep and comprehensive investigations.

3.2. Characterization of the porosity and tribo-mechanical behavior of the porous β-Ti substrates

In Fig. 4. a. as an example, the macro-structure of dense and porous β-Ti disks is presented; while, in Fig. 4b, a collage of the optical images is shown, in which the relatively homogeneous distribution of porosity can

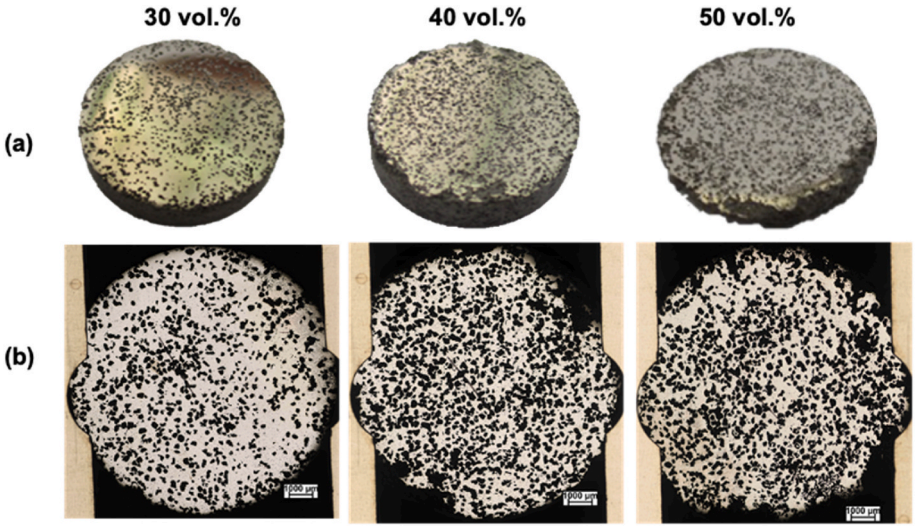

Fig. 4. a) Photograph of porous β-Ti disks, b) collage of optical microscopy images of the porous titanium substrates of β-Ti alloy.

be seen in the three types of disks manufactured by the spacer technique. Table 1 shows the density and the vol% of the porosity (total and interconnected) obtained; as well as details of the size (equivalent diameter) and morphology (shape factor) of the macro-pores inherent in the spacer. The analysis of these results verified that the spacer route is an economical and effective technique for reproducing and controlling the content and size of pores in metallic substrates. In addition, a direct relationship between the spacer content, the average size, and the irregularity of the resulting pores could be indicated, a fact that can be attributed to pore coalescence phenomena as their content increases.

Fig. 5 shows the static behavior (P-h curves) and the results derived for the 30 vol% and 40 vol% porous titanium substrates. In the case of the 50 vol% substrate, the instrumented micro-indentation curves obtained were not acceptable (irregular loading and unloading test). As expected, the maximum penetration, as well as the elastic recovery (absolute and relative) is greater for the more porous substrates. The analysis of the slopes of the curves during the unloading (Oliver and Pharr method), allowed us to estimate the values of HV and Young' modulus (E) for these two porous substrates: 30 vol%. (HV = 270 and E = 29 GPa) and 40 vol% (HV = 235 and E = 22 GPa). As expected, beta alloy's pores volumetric content is inversely proportional to stiffness and hardness values. Therefore, the pores content needed to be introduced into the implants, to replicate the mechanical requirements of cortical bone tissue (E = 20–25 GPa and σ_y = 150–180 MPa), is lower in implants made of the TNZT alloy (35 vol%), comparing with the required content in Ti c. p. (50 vol%). Another important characteristic of materials for orthopedic applications is the maximum elastic strain: for bones, it is approximately 1.1%, and for high-porosity TiNbZrTa samples it is approximately 3%, which guarantees that the implant will not be damaged before bone [62,63]. The hardness results are consistent with few studies reported in the literature (P-h curves), for dense beta titanium alloys [64,65]. It is interesting to note that the β-Ti alloy has a substantially higher hardness than cortical bone from femoral diaphysis [66].

The macro-mechanical behavior of dense Ti35Nb7Zr5Ta alloy has been reported in the literature (E = 55–64 GPa, σf = 265 MPa, σy = 480–530 MPa and UTS = 540–590 MPa) [47,54], while in porous β-Ti alloys [Ti-(18-20)Nb-(5-6)Zr] are limited. In this context, in the work of Brailovski et al. [53], the values of Young's modulus (uniaxial compression tests) of porous samples are reported to vary from 7.5 to 3.7 GPa and the maximum compression strength from 225 to 70 MPa, depending on porosity (from ~45 to 66%). These Young's modulus values from uniaxial compression tests are significantly lower than those from instrumented microindentation test. Some authors associated this discrepancy with super-elastic deformation within the linear-elastic range of tested materials [52]. In this same sense, the authors of this work have reported a similar trend for c. p. Ti obtained by a conventional powder-metallurgy process, as well as in works using space-holders (NaCl and NH_4HCO_3) [25,67–70]. These differences were attributed to a stiffness testing machine effect in which the mechanical system and the sample were considered to be two springs in series. Furthermore, note that the Ti matrix is different at each cross-section of the cylindrical sample during a compression test; the material collapse

Table 1
Characteristic parameters of the porosity obtained by the spacer route.

Spacer percentage	Archimedean Method			Image Analysis	
	ρ (g/cm^3)	P_T (%)	P_i (%)	D_{Eq} (μm)	*Ff*
30 vol%	3.93 ± 0.03	31.6 ± 0.5	21.8 ± 0.8	144 ± 30	0.59 ± 0.05
40 vol%	3.62 ± 0.15	37.0 ± 2.6	33.0 ± 2.5	155 ± 24	0.49 ± 0.07
50 vol %	3.37 ± 0.24	41.5 ± 4.1	39.2 ± 3.6	183 ± 32	0.50 ± 0.06

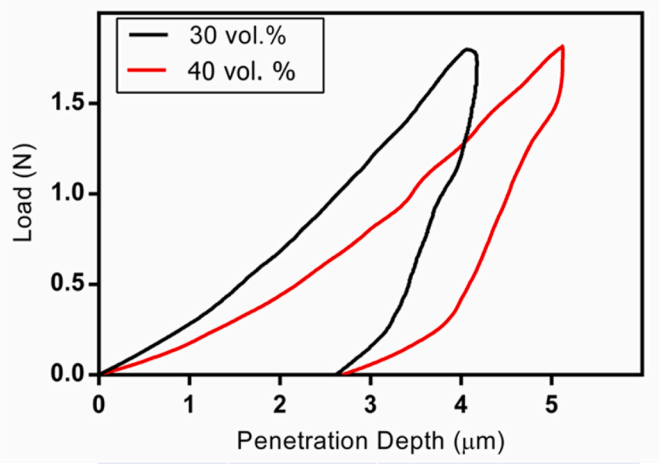

Substrate	Maximum Penetration depth (mm)	Elastic Recovery	
		Absolute (mm)	Relative (%)
30 vol.%	4.17 ± 0.03	2.61 ± 0.04	62.5 ± 0.2
40 vol.%	5.12 ± 0.05	2.68 ± 0.06	52.4 ± 0.3

Fig. 5. Mechanical behavior of the porous titanium substrates of the β-Ti alloy, loading-unloading curve (P-h curve). Note: the characteristic parameters of the curves are included in the table.

starts at the section with the lowest Ti content. In these works, the reliability and certainty of measurements were validated by comparison with well-known and accepted pore-elasticity models, such as that of Nielsen [71]. In this scenario, the mechanical properties measured in this work are more consistent with those reported in the literature for β-Ti alloys of similar composition and porosity.

The results of the scratch tests (Fig. 6) experienced a similar trend to that observed in the P-h curves, with the scratch resistance being lower (greater penetration depth and elastic recovery) in the β-Ti substrate with a 40 vol%. It is interesting to indicate the role of the macro-porosity in the roughness profile of the surface. In this sense, the values of R_a, R_q, R_z and R_y were lower in the less porous disk (see Fig. 7). In this same context, the clear increase in the roughness of the surface of the groove generated by the scratch test could be indicated, a fact that can be attributed to phenomena of deformation and collapse of the porous structure caused by imposed stress (see details in Fig. 8).

3.3. Bio-functional antibacterial behavior of PVA/PCL/AgNPs biocomposite

The combined use of two non-toxic, biocompatible polymers with different chemical nature, such as PCL and PVA in the appropriate proportions (50/50) has been shown to allow a controlled short-term release profile of therapeutic agents. This ratio was chosen based on a larger pore size of the biomaterial, with a larger surface area allowing for better degradation, and the drug release pattern was especially interesting, since the most frequent infections in implantology are described as occurring in the first 3 weeks after the intervention. The pharmaceutical goodness of this biomaterial with antibacterial action has been previously demonstrated, in a work recently published by the group of Prof. Torres, based on the Kirby-Bauer techniques and inhibition halo measurements, generated by samples when incubated on top on a bacterial lawn [24,72]. When the diameter of the generated halo was normalized with the diameter of the sample, the differences between samples could be semi qualitatively evaluated. Fig. 9 shows the antibacterial behavior of the composite against *P. aeruginosa* (Fig. 9 a) and *S. aureus* (Fig. 9 b), where the inhibition halos around the samples

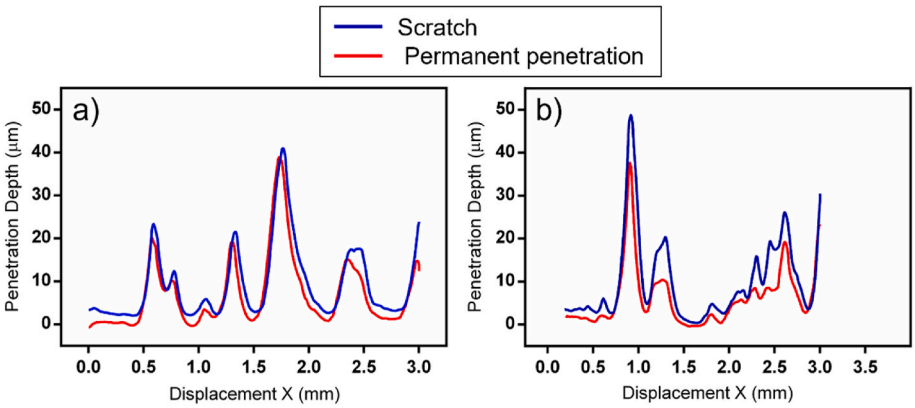

Fig. 6. In situ scratch tests and permanent penetration depth: a) 30 vol % b) 40 vol %.

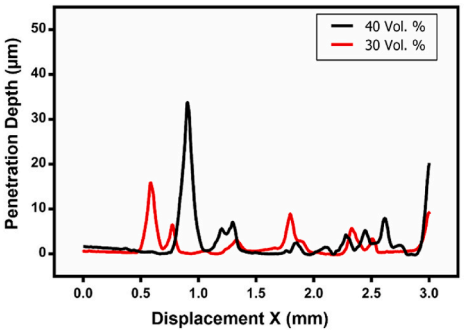

Sample		Ra	Rq	Rz	Ry
30 vol.%	Bare surface roughness	1.76	0.60	15.71	16.10
	Scratch groove roughness	7.13	0.69	38.25	39.65
40 vol.%	Bare surface roughness	2.81	1.66	33.55	34.01
	Scratch groove roughness	6.36	1.57	37.43	38.24

Fig. 7. Roughness profiles of the porous disks studied before coating (30 vol% and 40 vol%). Note: the characteristic roughness parameters (before and after the test) are included in the inset table.

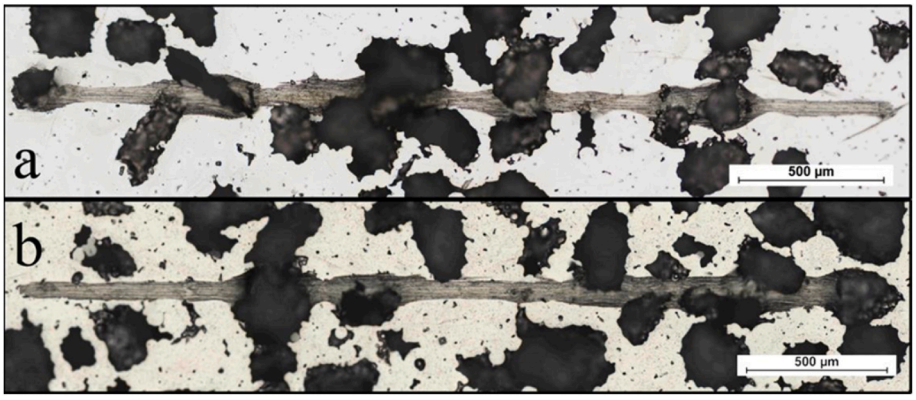

Fig. 8. Collage of optical images of the groove generated with the scratch test at constant load of 3 N and 3 mm scar length: a) 30 vol % b) 40 vol%.

can be clearly observed. This effect could be associated with the diffusion of both AgNPs and Ag^{+} over the TSA, preventing the seeded bacteria from proliferating. Where the antimicrobial agents could not reach, the bacterial lawn was visible. In this sense, the standardized value of the compiled halo was 1.71 ± 0.11 and 1.83 ± 0.26 for *P. aeruginosa* and *S. aureus*, respectively (Fig. 9 c). From these results, it could be concluded that both bacterial strains are sensitive to this composite, presenting slightly higher inhibition for S aureus.

3.4. Characterization of porous β-Ti substrates infiltrated with AgNPs-loaded composite biopolymer

The homogeneous mixture of the composite PVA/PCL/AgNPs was infiltrated into disks of the β-Ti TNZT alloy with different porosities (30, 40 and 50 vol%), as shown in Fig. 10. A comparison of the result of this infiltration of porous TNZT substrates with another previously prepared disk of c. p Ti 50 vol % porosity, was accomplished. Interestingly, it was observed an effect that concentrates part of the composite on the edges, reaching up to 3 mm in some cases.

This peculiar composite distribution was similar to a coffee ring-type pattern and generates an unexpected higher deposit of the coating on the perimeter when it dries. Interestingly, a slightly similar effect was observed when using c. p. Ti. The origin of this behavior might be related to different effects such as a) the disk size, b) the influence of the edge due to possible manufacturing irregularities, as those observed in the optical microscopy from images in Fig. 10a, c) the different chemical

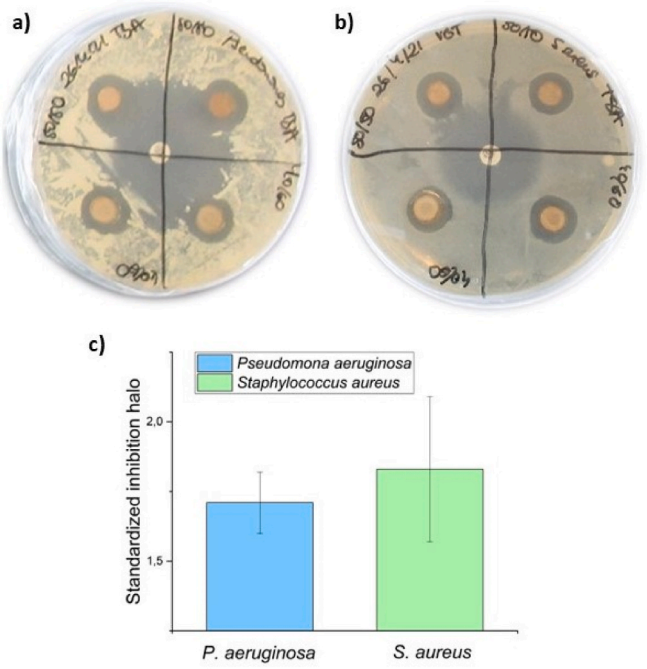

Fig. 9. Antimicrobial behavior of the composite. Inhibition halos generated by the composite when applying a modified version of the Kirby-Bauer diffusion method against a) *P. aeruginosa* and b) *S. aureus*. c) Values of the standardized halos.

composition (TNZT vs. c. p.Ti) of the metallic surface that would induce a hydrodynamic flow, d) to different interactions between the elements of the alloy and the components of the biopolymer coating, or perhaps e) to the chemical behavior of the heat shrink tube employed. In this context, it would be advisable to carry out XPS studies in future works to try to understand and/or explain in depth the possible causes. The use of surfactants, electrowettability, vibrations, or Marangoni fluxes may also be valued to minimize this effect.

In bone tissue regeneration, the ability of the implant to vascularize plays a fundamental role [73]. In this sense, there was an interesting phenomenon not only of interconnected porosity of β-Ti substrates, but also including the porosity of the polymer coating, with a pattern like honeycombs as observed in Fig. 11. In addition to the porosity of disks, an increase in porosity of coatings was observed, mainly generated by the presence of protuberances, whose content increased with larger pores of the β-Ti substrate. In this work, these protuberances could be identified as PVA considering the density of PCL (1.14 g/cm3) is lower than that of PVA (1.23 g/cm3), the latter can remain in greater proportion on the surface as it has greater difficulty infiltrating the macro-pores of the metal substrates). In this figure, the presence of a micro-porosity in the form of honeycomb inside the macro-pores of the substrate was also observed, like the morphology identified on the coating surface. In general, a detailed comparison pointed out that the porosity of the coating was more homogeneous in the coating deposited on the β-Ti substrate with 30 vol%.

Although a statistically significant trend cannot be established in relation to the size of the porosity of the coating, larger pores were observed in the coating on the substrate with a content of 40 vol% pores. This fact could be promoted by the kinetic evaporation of the solvent, which in this case could evaporate more abruptly, generating this surface orography.

In relation to the homogeneity and thickness of the polymeric coatings in the three types of porous substrates studied (Figs. 12 and 13), an inverse relationship could be indicated between the pore content of the metallic substrate, the thickness of the coating and the homogeneity of the material covering. The coating deposited on the substrate with a 50 vol% of pores was the thinnest and most heterogeneous. These facts can be attributed to the higher infiltration capacity of the biopolymer and the greater presence of PVA protuberances in the coating, respectively.

3.5. Surface wettability of disks with and without coatings

The effect of the macro-porosity of the porous β-Ti substrates and/or the biopolymeric coating (PVA/PCL/AgNPs) on the wettability behavior was studied. Wettability is a factor that can be related to the antibacterial behavior of a surface [74], such that a higher contact angle provides less wettability, which is related to greater hydrophobicity. Thus, a hydrophobic surface is more predisposed to inhibit the adhesion spread, and reproduction of bacteria of all kinds, and therefore, it is usually described as achieving superior antibacterial performance from a prophylactic point of view. The results shown in Fig. 14 indicated that when comparing the wettability of the dense β-Ti alloy with c. p. Ti, a significant increase in the contact angle of 25.2° was observed. This indicated interestingly that the new alloy offers a more hydrophobic surface and thus, potentially implemented features of bio-functionality. On the other hand, the wettability values of the infiltrated β-Ti substrates with different porosities are shown in Fig. 15. Unfortunately, it was not possible to obtain a wettability result for the porous substrate with 50 vol%, because the drop deposited on its surface quickly filtered into its interior. In general, two remarkable and very favorable trends were observed: 1) the increase in porosity implied a loss of the contact angle and, therefore, an increase in the hydrophilic character and 2) the coating with the biomaterial based on a polymeric matrix with embedded AgNPs provided an improvement in hydrophobicity values, regardless of the degree of porosity 30 or 40 vol%, being more

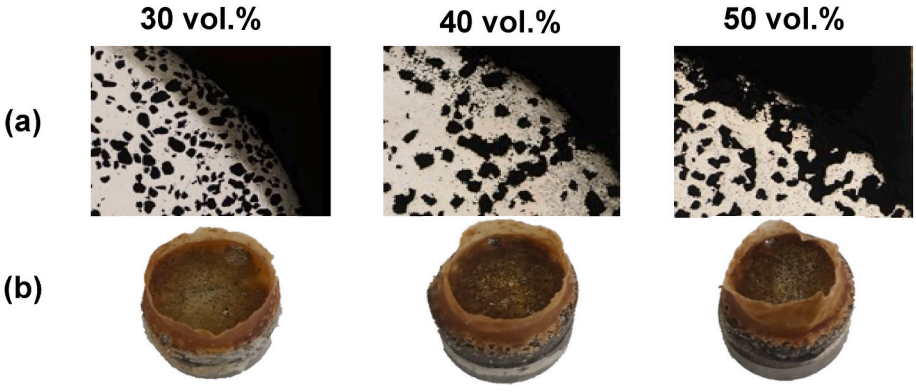

Fig. 10. a) Edges of the porous substrates of the β-Ti alloy (collapse and agglomerations of micropores), and b) Photograph of the porous disks of the β-Ti TNZT alloy, after the infiltration process of the composite biopolymer.

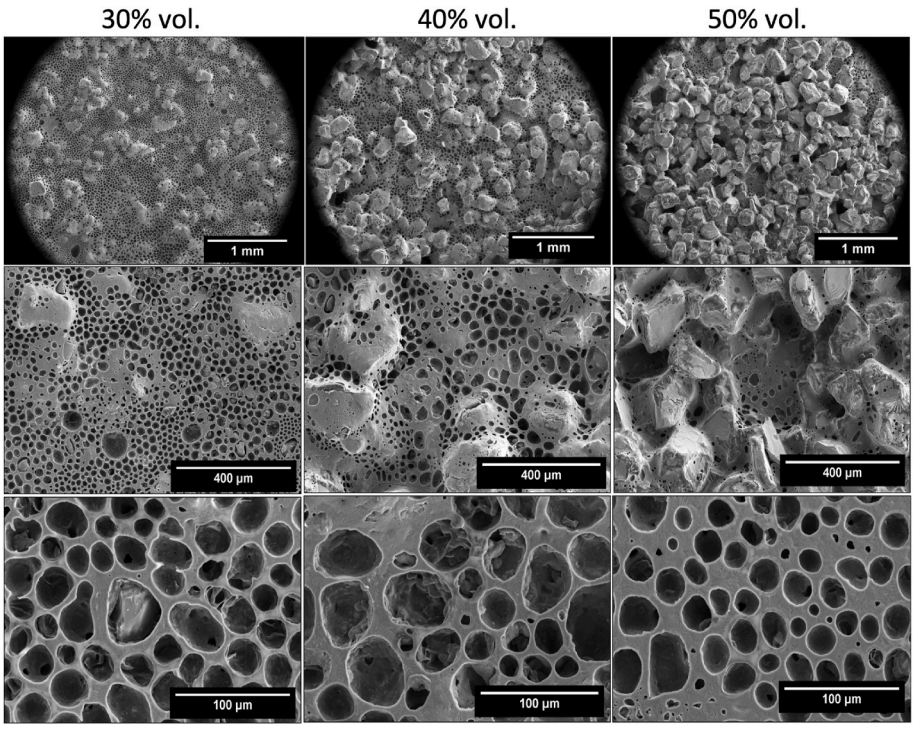

Fig. 11. Collage of SEM images at different magnifications of the coated titanium substrates from a top view.

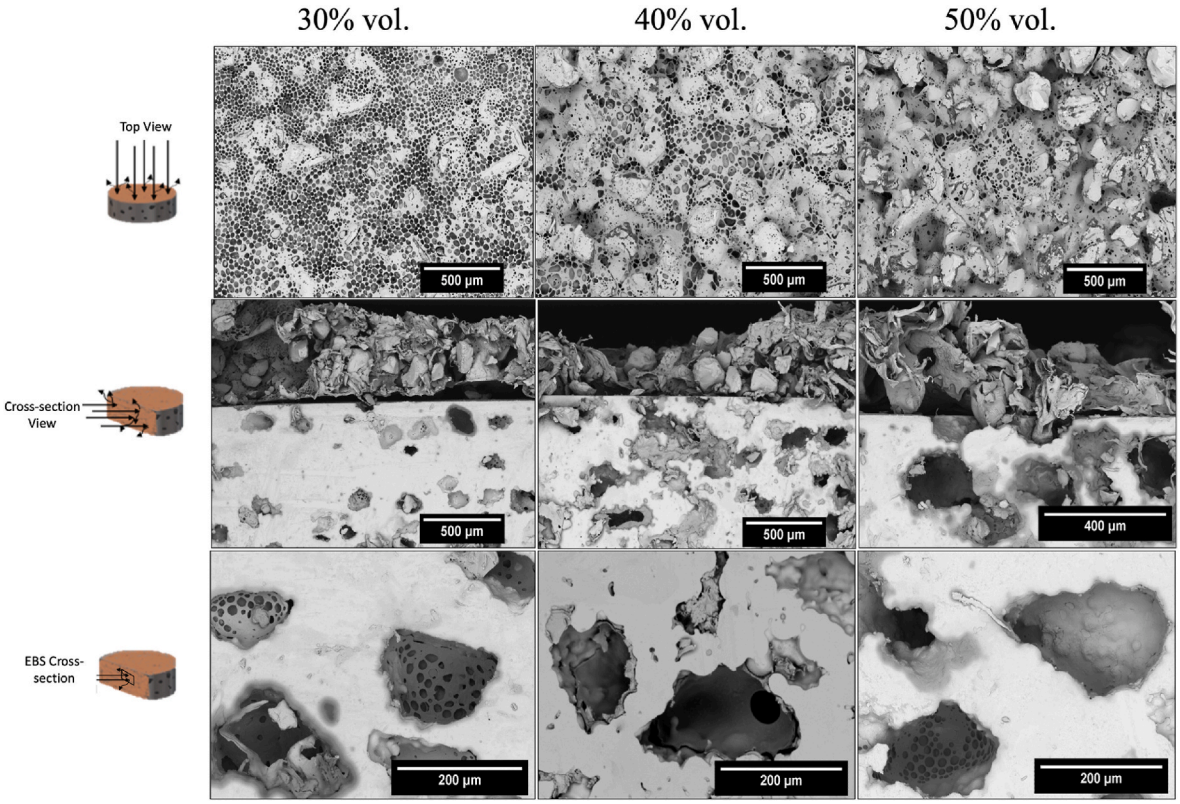

Fig. 12. Collage of BSE microscopy images of the coated porous titanium substrates. Top row: Infiltrated coating from top view. Intermediate row: Cross section where the level of infiltration and the thickness of the coating are observed. Lower row: Cross section at higher magnification where biopolymers are observed inside the macropores.

remarkable in the case of 40 vol%. In summary, the results indicated that the introduction of porosity in the metal and morphology of the coating positively influenced the solid-liquid contact of the Ti surface. The best bio-functionality could be achieved in our case with infiltrated substrates with 30 vol% porosity, thus providing a clear technical orientation for the design and application of metal porosities, which if combined with micro-textures with antibacterial properties could make a difference in the field of dental restoration.

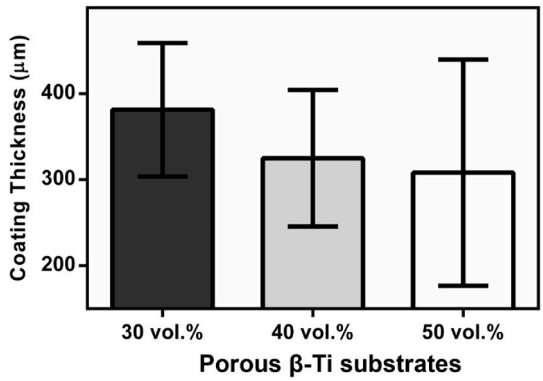

Fig. 13. Thicknesses of the biopolymeric PVA/PCL/AgNPs coatings on the surface of β-Ti porous substrates.

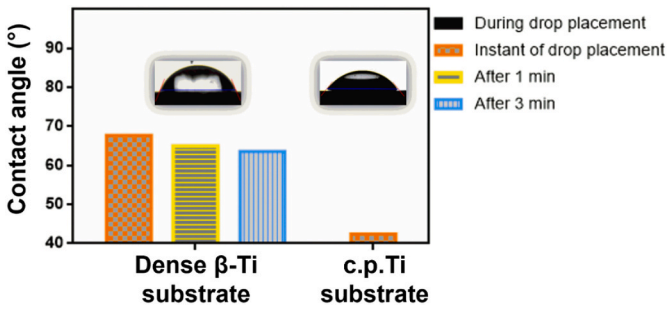

Fig. 14. Wettability values obtained for the β-Ti alloy and c. p. Ti.

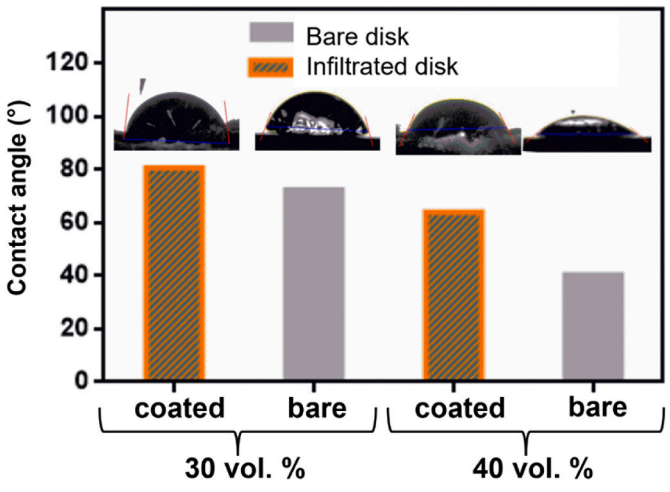

Fig. 15. Comparison of wettability values of porous β-Ti substrates infiltrated with biopolymer and bare porous disks, in porosities of 30 and 40 vol%.

4. Conclusions

In this study, different porous substrates of the β-Ti alloy (Ti35Nb7Zr5Ta) coated with a biopolymeric composite (PVA/PCL/AgNPs) have been manufactured and characterized, highlighting the good bio-mechanical and bio-functional balance obtained. Commercial powder had a spherical morphology and a rough surface. The powder particles presented a homogeneous chemical composition by weight corresponding to the beta alloy Ti35Nb7Zr5Ta. The compressibility of this material made it possible to obtain green compacts with good structural integrity before and after removing the spacer. The spacer technique was an economical, repetitive, and scalable manufacturing route on an industrial scale, allowing the control of the porosity (content and size of pores) of porous β-Ti alloys. Infiltration and coating of metal substrates with the antibacterial biocomposite PVA/PCL/AgNPs against *P. aeruginosa* and *S. aureus* were successful, although a "ring" effect was observed at the perimeter of the disks, which increased in size in the disks with greater porosity. The morphology and thickness of the layer in the different porous substrates of the β-Ti alloy showed that there was good penetration of the material, producing different orographies on the surface. On the other hand, the smallest thickness corresponded to the largest porosity. In addition, the wettability study showed that this alloy was more hydrophobic (potentially with better bio-functionality characteristics), compared to that of Ti c. p.; additionally, the comparison of porosity indicated that with the less porosity 30 vol% the surface would potentially induce better antibacterial behavior.

CRediT authorship contribution statement

Ernesto J. Delgado-Pujol: Data curation, Formal analysis, Investigation, Validation, Roles/. **Ana Alcudia:** Conceptualization, Funding acquisition, Investigation, Methodology, Project administration, Resources, Supervision, Visualization, Roles/. **Amir A. Elhadad:** Conceptualization, Data curation, Formal analysis, Investigation, Methodology, Software, Supervision, Validation, Visualization, Roles/. **Luisa Marleny Rodríguez-Albelo:** Conceptualization, Data curation, Formal analysis, Investigation, Methodology, Resources, Software, Supervision, Validation, Visualization, Roles/. **Paula Navarro:** Conceptualization, Data curation, Formal analysis, Investigation, Methodology, Software, Supervision, Validation, Visualization, Roles/. **Belén Begines:** Conceptualization, Data curation, Formal analysis, Funding acquisition, Investigation, Methodology, Project administration, Resources, Software, Supervision, Validation, Visualization, Roles/. **Yadir Torres:** Conceptualization, Funding acquisition, Investigation, Methodology, Project administration, Resources, Supervision, Visualization, Roles/.

Declaration of competing interest

The authors declare that they have no known competing financial interests or personal relationships that could have appeared to influence the work reported in this paper.

Data availability

Data will be made available on request.

Acknowledgments

This work was supported by the Ministry of Science and Innovation of Spain [grant number PID2019-109371 GB-I00], by the Junta de Andalucía (Spain) through the Projects, PAIDI [grant Ref. P20_00671], and FEDER Andalucía, grant number US-1380878. Also, it was funded by Universidad de Sevilla, through VII Plan Propio de Investigación y Transferencia-US 2022, grant numbers: 2022/00000332 and 2022/00000277; A.A.E. thanks for a María Zambrano Requalification Contract. The authors also would like to thank the investigation support of technician J. Pinto for the contribution to the tribo-mechanical characterization.

References

[1] E. Bernabe, W. Marcenes, C.R. Hernandez, J. Bailey, L.G. Abreu, V. Alipour, S. Amini, J. Arabloo, Z. Arefi, A. Arora, M.A. Ayanore, T.W. Bärnighausen, A. Bijani, D.Y. Cho, D.T. Chu, C.S. Crowe, G.T. Demoz, D.G. Demsie, Z.S. Dibaji Forooshani, M. Du, M. El Tantawi, F. Fischer, M.O. Folayan, N.D. Futran, Y.C. D. Geramo, A. Haj-Mirzaian, N. Hariyani, A. Hasanzadeh, S. Hassanipour, S.I. Hay, M.K. Hole, S. Hostiuc, M.D. Ilic, S.L. James, R. Kalhor, L. Kemmer, M. Keramati, Y. S. Khader, S. Kisa, A. Kisa, A. Koyanagi, R. Lalloo, Q. Le Nguyen, S.D. London, N. D. Manohar, B.B. Massenburg, M.R. Mathur, H.G. Meles, T. Mestrovic, A. Mohammadian-Hafshejani, R. Mohammadpourhodki, A.H. Mokdad, S.

D. Morrison, J. Nazari, T.H. Nguyen, C.T. Nguyen, M.R. Nixon, T.O. Olagunju, K. Pakshir, M. Pathak, N. Rabiee, A. Rafiei, K. Ramezanzadeh, M.J. Rios-Blancas, E. M. Roro, S. Sabour, A.M. Samy, M. Sawhney, F. Schwendicke, F. Shaahmadi, M. A. Shaikh, C. Stein, M.R. Tovani-Palone, B.X. Tran, B. Unnikrishnan, G.T. Vu, A. Vukovic, T.S.S. Warouw, Z. Zaidi, Z.J. Zhang, N.J. Kassebaum, Global, regional, and national levels and trends in burden of oral conditions from 1990 to 2017: a systematic analysis for the global burden of disease 2017 study, J. Dent. Res. 99 (4) (2020) 362–373, https://doi.org/10.1177/0022034520908533.

[2] Anna Gościniak, Magdalena Paczkowska-Walendowska, Agnieszka Skotnicka, Marek A. Ruchała, Judyta Cielecka-Piontek, Can plant materials Be valuable in the treatment of periodontal diseases? Practical review, Pharmaceutics 13 (12) (2021) 2185, https://doi.org/10.3390/pharmaceutics13122185.

[3] Leszek A. Dobrzański, Lech B. Dobrzański, Anna D. Dobrzańska-Danikiewicz, Joanna Dobrzańska, The concept of sustainable development of modern dentistry, Processes 8 (12) (2020) 1605, https://doi.org/10.3390/pr8121605.

[4] Luting Liu, Thomas J. Webster, Nanotechnology for reducing orthopedic implant infections: synthesis, characterization, and properties, in: Orthopedic Biomaterials, Springer, 2017, pp. 31–62. https://link.springer.com/content/pdf/10.1007/978-3-319-73664-8.pdf.

[5] Fernando G. Oliveira, Ana R. Ribeiro, Geronimo Perez, Bráulio S. Archanjo, Cristol P. Gouvea, Joyce R. Araújo, Andrea PC. Campos, Alexei Kuznetsov, Clara M. Almeida, Márcia M. Maru, Understanding growth mechanisms and tribocorrosion behaviour of porous Tio2 anodic films containing calcium, phosphorous and magnesium, Appl. Surf. Sci. 341 (2015) 1–12, https://doi.org/10.1016/j.apsusc.2015.02.163.

[6] Tara Renton, Dental (odontogenic) pain, Reviews in pain 5 (1) (2011) 2–7, https://doi.org/10.1177/204946371100500102.

[7] Jainara Maria Soares Ferreira, Ednara Mercia Fernandes de Andrade, Cíntia Regina Tornisiello Katz, Aronita Rosenblatt, Prevalence of dental trauma in deciduous teeth of Brazilian children, Dent. Traumatol. 25 (2) (2009) 219–223, https://doi.org/10.1111/j.1600-9657.2008.00754.x.

[8] Steve Kisely, No mental health without oral health, Can. J. Psychiatr. 61 (5) (2016) 277–282, https://doi.org/10.1177/0706743716632523.

[9] Tatiane Martins Jorge, Ana Karolina Zampronio Bassi, Sérgio Donha Yarid, Henrique Mendes Silva, Ricardo Pianta Rodrigues da Silva, Magali de Lourdes Caldana, José Roberto de Magalhães Bastos, Relation between tooth loss and chewing, swallowing and speech complaints in adults, Revista CEFAC 11 (2009) 391–397, https://doi.org/10.1590/S1516-18462009000700015.

[10] Nikki Rousseau, Jimmy Steele, Carl May, Catherine Exley, 'Your whole life is lived through your teeth': biographical disruption and experiences of tooth loss and replacement, Sociol. Health Illness 36 (3) (2014) 462–476, https://doi.org/10.1111/1467-9566.12080.

[11] Peng Du, Tao Xiang, Xinxin Yang, Guoqiang Xie, Enhanced mechanical and antibacterial properties of Cu-bearing Ti-based bulk metallic glass by controlling porous structure, J. Alloys Compd. 904 (2022), 164005, https://doi.org/10.1016/j.jallcom.2022.164005.

[12] Amit Mahajan, Gurpreet Singh, Sandeep Devgan, Sarabjeet Singh Sidhu, Edm performance characteristics and electrochemical corrosion analysis of Co-Cr alloy and duplex stainless steel: a comparative study, Proc. IME E J. Process Mech. Eng. 235 (4) (2021) 812–823, https://doi.org/10.1177/0954408920976739.

[13] Naoya Taniguchi, Shunsuke Fujibayashi, Mitsuru Takemoto, Kiyoyuki Sasaki, Bungo Otsuki, Takashi Nakamura, Tomiharu Matsushita, Tadashi Kokubo, Shuichi Matsuda, Effect of pore size on bone ingrowth into porous titanium implants fabricated by additive manufacturing: an in vivo experiment, Mater. Sci. Eng. C 59 (2016) 690–701, https://doi.org/10.1016/j.msec.2015.10.069.

[14] Bruna C. Costa, Cíntia K. Tokuhara, Luís A. Rocha, Rodrigo C. Oliveira, Paulo N. Lisboa-Filho, João Costa Pessoa, Vanadium ionic species from degradation of Ti-6al-4v metallic implants: in vitro cytotoxicity and speciation evaluation, Mater. Sci. Eng. C 96 (2019) 730–739, https://doi.org/10.1016/j.msec.2018.11.090.

[15] V.S.A. Challa, S. Mali, R.D.K. Misra, Reduced toxicity and superior cellular response of preosteoblasts to Ti-6al-7nb alloy and comparison with Ti-6al-4v, J. Biomed. Mater. Res. 101 (7) (2013) 2083–2089, https://doi.org/10.1002/jbm.a.34492.

[16] Krzysztof Rokosz, Tadeusz Hryniewicz, Steinar Raaen, Development of plasma electrolytic oxidation for improved Ti6al4v biomaterial surface properties, Int. J. Adv. Manuf. Technol. 85 (9) (2016) 2425–2437, https://doi.org/10.1007/s00170-015-8086-y.

[17] Fabian Haase, Carsten Siemers, Lina Klinge, Cheng Lu, Patric Lang, Stephan Lederer, König Till, Joachim Rösler, Aluminum-and vanadium-free titanium alloys for medical applications, Paper presented at the MATEC Web of Conferences, https://doi.org/10.1051/matecconf/202032105008, 2020.

[18] Peter K. Moy, Diana Medina, Vivek Shetty, Tara L. Aghaloo, Dental implant failure rates and associated risk factors, Int. J. Oral Maxillofac. Implants 20 (4) (2005). PMID: 16161741.

[19] Yadir Torres, Perla Sarria, Francisco José Gotor, Eliel Gutiérrez, Eduardo Peon, Ana María Beltrán, Jesús E. González, Surface modification of Ti-6al-4v alloys manufactured by selective laser melting: microstructural and tribo-mechanical characterization, Surf. Coating. Technol. 348 (2018) 31–40, https://doi.org/10.1016/j.surfcoat.2018.05.015.

[20] E. Yılmaz, A. Gökçe, F. Findik, H.O. Gulsoy, O. İyibilgin, Mechanical properties and electrochemical behavior of porous Ti-Nb biomaterials, J. Mech. Behav. Biomed. Mater. 87 (2018) 59–67, https://doi.org/10.1016/j.jmbbm.2018.07.018.

[21] Minqi Wang, Tingting Tang, Surface treatment strategies to combat implant-related infection from the beginning, J. Orthopaed. Translat. 17 (2019) 42–54, https://doi.org/10.1016/j.jot.2018.09.001.

[22] Erlin Zhang, Xiaotong Zhao, Jiali Hu, Ruoxian Wang, Shan Fu, Gaowu Qin, Antibacterial metals and alloys for potential biomedical implants, Bioact. Mater. 6 (8) (2021) 2569–2612, https://doi.org/10.1016/j.bioactmat.2021.01.030.

[23] Eren Yılmaz, Azim Gökçe, Fehim Findik, HOzkan Gulsoy, Metallurgical properties and biomimetic HA deposition performance of Ti-Nb PIM alloys, J. Alloys Compd. 746 (2018) 301–313, https://doi.org/10.1016/j.jallcom.2018.02.274.

[24] Ana Alcudia, Belén Begines, Paula Rodriguez-Lejarraga, Valeria Greyer, Vanda Cristina Fortio Godinho, Eloísa Pajuelo, Yadir Torres, Development of porous silver nanoparticle/polycaprolactone/polyvinyl alcohol coatings for prophylaxis in titanium interconnected samples for dental implants, Colloid Interface Sci. Commun. 48 (2022), 100621, https://doi.org/10.1016/j.colcom.2022.100621.

[25] Sheila Lascano, Cristina Arévalo, Isabel Montealegre-Melendez, Sergio Muñoz, José A. Rodriguez-Ortiz, Paloma Trueba, Yadir Torres, Porous titanium for biomedical applications: evaluation of the conventional powder metallurgy frontier and space-holder technique, Appl. Sci. 9 (5) (2019) 982, https://doi.org/10.3390/app9050982.

[26] Naim Aslan, B. Aksakal, F. Findik, Fabrication of porous-Ti6Al4V alloy by using hot pressing technique and Mg space holder for hard-tissue biomedical applications, J. Mater. Sci. Mater. Med. 32 (7) (2021) 80, https://doi.org/10.1007/s10856-021-06546-2.

[27] Bowen Liu, Wei Xu, Xin Lu, Maryam Tamaddon, Mingying Chen, Jiaqi Dong, Yitong Liu, Lijia Guo, Jiazhen Zhang, Xuanhui Qu, Xinbo He, Chaozong Liu, The optimization of Ti gradient porous structure involves the finite element simulation analysis, Front. Mater. 8 (2021), https://doi.org/10.3389/fmats.2021.642135.

[28] Cristina Domínguez-Trujillo, Fátima Ternero, José Antonio Rodríguez-Ortiz, Juan José Pavón, Isabel Montealegre-Meléndez, Cristina Arévalo, Francisco García-Moreno, Yadir Torres, Improvement of the balance between a reduced stress shielding and bone ingrowth by bioactive coatings onto porous titanium substrates, Surf. Coating. Technol. 338 (2018) 32–37, https://doi.org/10.1016/j.surfcoat.2018.01.019.

[29] Eren Yılmaz, Bekir Çakıroğlu, Azim Gökçe, Fehim Findik, H Ozkan Gulsoy, Nagihan Gulsoy, Özal Mutlu, Mahmut Özacar, Novel hydroxyapatite/graphene oxide/collagen bioactive composite coating on Ti16Nb alloys by electrodeposition, Mater. Sci. Eng. C 101 (2019) 292–305, https://doi.org/10.1016/j.msec.2019.03.078.

[30] Anwesha Barik, Nishant Chakravorty, Targeted drug delivery from titanium implants: a review of challenges and approaches, Trends Biomed. Res. (2019) 1–17, https://doi.org/10.1007/5584_2019_447.

[31] Ana M. Beltrán, Ana Civantos, Cristina Dominguez-Trujillo, Rocío Moriche, José A. Rodríguez-Ortiz, Francisco García-Moreno, Thomas J. Webster, Paul H. Kamm, Andrea mesa restrepo, and Yadir torres. "Porous titanium surfaces to control bacteria growth: mechanical properties and sulfonated polyetheretherketone coatings as antibiofouling approaches, Metals 9 (9) (2019) 995, https://doi.org/10.3390/met9090995.

[32] Steven L. Percival, John Thomas, Sara Linton, Okel Tyler, Linda Corum, Will Slone, The antimicrobial efficacy of silver on antibiotic-resistant bacteria isolated from burn wounds, Int. Wound J. 9 (5) (2012) 488–493, https://doi.org/10.1111/j.1742-481X.2011.00903.x.

[33] Shaoheng Tang, Jie Zheng, Antibacterial activity of silver nanoparticles: structural effects, Adv. Healthcare Mater. 7 (13) (2018), 1701503, https://doi.org/10.1002/adhm.201701503.

[34] Romero-Urbina, G. Dulce, Humberto H. Lara, J Jesús Velázquez-Salazar, M Josefina Arellano-Jiménez, Eduardo Larios, Anand Srinivasan, Jose L. Lopez-Ribot, Miguel José Yacamán, Ultrastructural changes in methicillin-resistant Staphylococcus aureus induced by positively charged silver nanoparticles, Beilstein J. Nanotechnol. 6 (1) (2015) 2396–2405, https://doi.org/10.3762/bjnano.6.246.

[35] Anna Kędziora, Mateusz Speruda, Eva Krzyżewska, Jacek Rybka, Łukowiak Anna, Gabriela Bugla-Płoskońska, Similarities and differences between silver ions and silver in nanoforms as antibacterial agents, Int. J. Mol. Sci. 19 (2) (2018) 444, https://doi.org/10.3390/ijms19020444.

[36] Nelson Durán, Marcela Durán, Marcelo Bispo de Jesus, Amedea B. Seabra, Wagner J. Fávaro, Gerson Nakazato, Silver nanoparticles: a new view on mechanistic aspects on antimicrobial activity, Nanomed. Nanotechnol. Biol. Med. 12 (3) (2016) 789–799, https://doi.org/10.1016/j.nano.2015.11.016.

[37] G.M. Esteves, J. Esteves, M. Resende, L. Mendes, A.S. Azevedo, Antimicrobial and antibiofilm coating of dental implants-past and new perspectives, Antibiotics 11 (2) (2022), https://doi.org/10.3390/antibiotics11020235.

[38] Mariana Prodana, Andrei Bogdan Stoian, Cristian Burnei, Daniela Ionita, Innovative coatings of metallic alloys used as bioactive surfaces in implantology: a review, Coatings 11 (6) (2021) 649, https://doi.org/10.3390/coatings11060649.

[39] A Joseph Nathanael, Tae Hwan Oh, Biopolymer coatings for biomedical applications, Polymers 12 (12) (2020) 3061, https://doi.org/10.3390/polym12123061.

[40] B. Priyadarshini, M. Rama, Chetan, U. Vijayalakshmi, Bioactive coating as a surface modification technique for biocompatible metallic implants: a review, J. Asian Ceramic Soc. 7 (4) (2019) 397–406, https://doi.org/10.1080/21870764.2019.1669861.

[41] E. Olewnik-Kruszkowska, M. Gierszewska, E. Jakubowska, I. Tarach, V. Sedlarik, M. Pummerova, Antibacterial films based on pva and pva-chitosan modified with poly(hexamethylene guanidine), Polymers 11 (12) (2019), https://doi.org/10.3390/polym11122093.

[42] A Sandeep Kranthi Kiran, TS Sampath Kumar, Rutvi Sanghavi, Mukesh Doble, Seeram Ramakrishna, Antibacterial and bioactive surface modifications of titanium implants by pcl/tio2 nanocomposite coatings, Nanomaterials 8 (10) (2018) 860, https://doi.org/10.3390/nano8100860.

[43] Neha Raina, Rakesh Pahwa, Jasmine Kour Khosla, Prem N. Gupta, Madhu Gupta, Polycaprolactone-based materials in wound healing applications, Polym. Bull. (2021) 1–23, https://doi.org/10.1007/s00289-021-03865-w.
[44] S. Nag, R. Banerjee, H.L. Fraser, A Novel combinatorial approach for understanding microstructural evolution and its relationship to mechanical properties in metallic biomaterials, Acta Biomater. 3 (3) (2007) 369–376, https://doi.org/10.1016/J.ACTBIO.2006.08.005.
[45] Mohsin Talib Mohammed, Zahid A. Khan, Arshad N. Siddiquee, Beta titanium alloys: the lowest elastic modulus for biomedical applications: a review, Int. J. Chem. Mol. Nucl. Mater. Metall. Eng 8 (8) (2014) 726, https://doi.org/10.5281/zenodo.1094481.
[46] Marc Long, H.J. Rack, Titanium alloys in total joint replacement—a materials science perspective, Biomaterials 19 (18) (1998) 1621–1639, https://doi.org/10.1016/S0142-9612(97)00146-4.
[47] R.P. Kolli, A. Devaraj, A review of metastable beta titanium alloys, Metals 8 (1–41) (2018), https://doi.org/10.3390/met8070506.
[48] Sarabjeet Singh Sidhu, Harpreet Singh, Mohamed Abdel-Hady Gepreel, A review on alloy design, biological response, and strengthening of β-titanium alloys as biomaterials, Mater. Sci. Eng. C 121 (2021), 111661, https://doi.org/10.1016/j.msec.2020.111661.
[49] E D Velten Eisenbarth, M. Müller, R. Thull, J. Breme, Biocompatibility of β-stabilizing elements of titanium alloys, Biomaterials 25 (26) (2004) 5705–5713, https://doi.org/10.1016/j.biomaterials.2004.01.021.
[50] Mitsuo Niinomi, Mechanical biocompatibilities of titanium alloys for biomedical applications, J. Mech. Behav. Biomed. Mater. 1 (1) (2008) 30–42, https://doi.org/10.1016/j.jmbbm.2007.07.001.
[51] E. Sallica-Leva, Jardini Al, J.B. Fogagnolo, Microstructure and mechanical behavior of porous Ti–6al–4v parts obtained by selective laser melting, J. Mech. Behav. Biomed. Mater. 26 (2013) 98–108, https://doi.org/10.1016/j.jmbbm.2013.05.011.
[52] Mitsuo Niinomi, Masaaki Nakai, Junko Hieda, Development of new metallic alloys for biomedical applications, Acta Biomater. 8 (11) (2012) 3888–3903, https://doi.org/10.1016/j.actbio.2012.06.037.
[53] Vladimir Brailovski, S. Prokoshkin, Gauthier M, K. Inaekyan, S. Dubinskiy, M. Petrzhik, M. Filonov, Bulk and porous metastable beta Ti–Nb–Zr (Ta) alloys for biomedical applications, Mater. Sci. Eng. C 31 (3) (2011) 643–657, https://doi.org/10.1016/j.msec.2010.12.008.
[54] Weitian Zhao, David Michalik, Stephen Ferguson, Willy Hofstetter, Jacques Lemaître, Brigitte von Rechenberg, Bowen Paul, Rapid evaluation of bioactive Ti-based surfaces using an in vitro titration method, Nat. Commun. 10 (1) (2019) 1–11, https://doi.org/10.1038/s41467-019-09673-1.
[55] Colin McPhee, Jules Reed, Izaskun Zubizarreta, Wettability and wettability tests, in: Developments in Petroleum Science, vols. 313–45, Elsevier, 2015, https://doi.org/10.1016/B978-0-444-63533-4.00007-X.
[56] Ian N. Sneddon, The relation between load and penetration in the axisymmetric boussinesq problem for a punch of arbitrary profile, Int. J. Eng. Sci. 3 (1) (1965) 47–57, https://doi.org/10.1016/0020-7225(65)90019-4.
[57] Warren Carl Oliver, George Mathews Pharr, An improved technique for determining hardness and elastic modulus using load and displacement sensing indentation experiments, J. Mater. Res. 7 (6) (1992) 1564–1583, https://doi.org/10.1557/JMR.1992.1564.
[58] Warren C. Oliver, Georges M. Pharr, Measurement of hardness and elastic modulus by instrumented indentation: advances in understanding and refinements to methodology, J. Mater. Res. 19 (1) (2004) 3–20, https://doi.org/10.1557/jmr.2004.19.1.3.
[59] C-05, Astm, Standard Test Method for Adhesion Strength and Mechanical Failure Modes of Ceramic Coatings by Quantitative Single Point Scratch Testing, 2005, https://doi.org/10.1520/C1624-05.
[60] Ragaseema V. Madhavan, Mathirappillil J. Rosemary, Maya A. Nandkumar, Kalliyana V. Krishnan, Lissy K. Krishnan, Silver nanoparticle impregnated poly (ε-Caprolactone) scaffolds: optimization of antimicrobial and noncytotoxic concentrations, Tissue Eng. 17 (3–4) (2011), https://doi.org/10.1089/ten.tea.2009.0791, 439-49.
[61] Clinical, L.S. Institute, in: Clsi (Ed.), Perfomance Standards for Antimicrobial Disk Susceptibility Tests, thirteenth ed., Clinical and Laboratory Standards Institute, Wayne, Pa, 2018. **ISBN Number:**978-1-68440-135-2.
[62] Rodolfo Lisboa Batalha, Weverson Capute Batalha, Liang Deng, Tobias Gustmann, Pauly Simon, Claudio Shyinti Kiminami, Piter Gargarella, Processing a biocompatible Ti–35nb–7zr–5ta alloy by selective laser melting, J. Mater. Res. 35 (9) (2020) 1143–1153, https://doi.org/10.1557/jmr.2020.90.
[63] Tara L Arthur Moore, Microdamage accumulation in bovine trabecular bone. Massachusetts institute of technology, J. Biomech. Eng. 124 (2001) 63–71, https://doi.org/10.1115/1.1428745.
[64] T. Maity, C Gammer Ö Balcı, E. Ivanov, J. Eckert, K.G. Prashanth, High pressure torsion induced lowering of Young's modulus in high strength TNZT alloy for bio-implant applications, J. Mech. Behav. Biomed. Mater. 108 (2020), 103839, https://doi.org/10.1016/j.jmbbm.2020.103839 (Get rights and content).
[65] Xueyang Zhao, Peng Zhang, Xiaojian Wang, Yun Chen, Hui Liu, Lianxi Chen, Yinying Sheng, Wei Li, In-situ formation of textured tin coatings on biomedical titanium alloy by laser irradiation, J. Mech. Behav. Biomed. Mater. 78 (2018) 143–153, https://doi.org/10.1016/j.jmbbm.2017.11.019.
[66] Robert C. Singleton, George M. Pharr, Jeffry S. Nyman, Increased tissue-level storage modulus and hardness with age in male cortical bone and its association with decreased fracture toughness, Bone 148 (2021), 115949, https://doi.org/10.1016/j.bone.2021.115949.
[67] Yadir Torres, J.J. Pavón, I. Nieto, J.A. Rodríguez, Conventional powder metallurgy process and characterization of porous titanium for biomedical applications, Metall. Mater. Trans. B 42 (2011) 891–900, https://doi.org/10.1007/s11663-011-9521-6.
[68] Yadir Torres, Sheila Lascano, Jorge Bris, Pavón Juan, José A. Rodriguez, Development of porous titanium for biomedical applications: a comparison between loose sintering and space-holder techniques, Mater. Sci. Eng. C 37 (2014) 148–155, https://doi.org/10.1016/j.msec.2013.11.036.
[69] Y. Torres, J.J. Pavón, J.A. Rodríguez, Processing and characterization of porous titanium for implants by using nacl as space holder, J. Mater. Process. Technol. 212 (5) (2012) 1061–1069, https://doi.org/10.1016/j.jmatprotec.2011.12.015.
[70] J.J. Pavón, P. Trueba, J.A. Rodríguez-Ortiz, Y. Torres, Development of new titanium implants with longitudinal gradient porosity by space-holder technique, J. Mater. Sci. 50 (2015) 6103–6112, https://doi.org/10.1007/s10853-015-9163-1.
[71] Nielsen, Fuglsang Lauge, Elasticity and damping of porous materials and impregnated materials, J. Am. Ceram. Soc. 67 (2) (1984) 93–98, https://doi.org/10.1111/j.1151-2916.1984.tb09622.x.
[72] Makabenta, V. Jessa Marie, Nabawy Ahmed, Cheng-Hsuan Li, Suzannah Schmidt-Malan, Robin Patel, Vincent M. Rotello, Nanomaterial-based therapeutics for antibiotic-resistant bacterial infections, Nat. Rev. Microbiol. 19 (1) (2021) 23–36, https://doi.org/10.1038/s41579-020-0420-1.
[73] Marina I. Santos, Rui L. Reis, Vascularization in bone tissue engineering: physiology, current strategies, major hurdles and future challenges, Macromol. Biosci. 10 (1) (2010) 12–27, https://doi.org/10.1002/mabi.200900107.
[74] Jinyang Xu, Min Ji, Linfeng Li, Yi Wu, Yu Qi, Ming Chen, Improving wettability, antibacterial and tribological behaviors of zirconia ceramics through surface texturing, Ceram. Int. 48 (3) (2022) 3702–3710, https://doi.org/10.1016/j.ceramint.2021.10.152.